16TH EUROPEAN CONFERENCE ON EARTHQUAKE ENGINEERING THESSALONIKI 18 - 21 JUNE 2018

USING THE APPLIED ELEMENT METHOD TO SIMULATE THE DYNAMIC RESPONSE OF FULL-SCALE URM HOUSES TESTED TO COLLAPSE OR NEAR-COLLAPSE CONDITIONS

Daniele MALOMO[1], Rui PINHO[1,2], Andrea PENNA[1,3]

ABSTRACT

In this work, the Applied Element Method (AEM) is employed to reproduce the dynamic response of three full-scale unreinforced masonry (URM) house specimens tested on a shake-table. Two of the test specimens correspond to a calcium-silicate terraced house typology (typical of construction in the Netherlands and other Northern European countries), whilst a third one corresponds to a clay masonry detached house (representative not only of Northern Europe construction typologies, but also of houses found in other regions of the world, such as Australia and New Zealand). The test specimens were subjected to dynamic inputs of increasing intensity, both for reasons of shake-table control as well as for monitoring of progressive damage/limit states evolution. For two of the specimens, near collapse conditions were reached during their testing, whilst for the third an explicit structural collapse was obtained.

Keywords: applied element method; discrete elements modelling; unreinforced masonry; shake-table testing

1. INTRODUCTION

The construction culture and practice in the until recently non-seismic Groningen region, now subjected to induced seismicity due to natural gas extraction, is understandably and naturally distinct from what is typically found in areas of the world that have a long history of damaging earthquakes. As such, neither experimental data nor verified numerical models for the characterisation of the seismic response of these types of structures were available in the literature, the reason for which an extensive research programme aimed at addressing such knowledge gap was deployed, under the sponsorship of the Nederlandse Aardolie Maatschappij BV (NAM).

Such research programme featured a number of workstreams, described in van Elk et al. (2018), including laboratory testing of a number of unreinforced masonry (URM) and reinforced concrete (RC) full-scale test specimens. Of particular relevance to the work described herein is the shake-table testing of two calcium-silicate terraced house specimens, as well as of a clay masonry detached house. For each of these full-scale tests, a number of teams, each of which using different modelling approaches, were invited to carry out, first, blind-predictions of the tests results, and then calibrated "post-dictions" (e.g. Arup et al. 2015, 2017); such numerical validation endeavour lent confidence and reassurance to the process through which the analytical fragility functions for the Groningen region was developed (Crowley et al. 2017, Crowley and Pinho, 2017), since it was based on detailed nonlinear dynamic analyses of representative buildings (Arup 2017, Mosayk 2017a).

In this paper, the employment of the Applied Element Method (Meguro and Tagel-Din, 2000, 2001, 2002) in such cross-modelling validation exercise is described, showing how this relatively recent addition to the discrete elements methods family has the capability of producing reliable estimation of the response of URM buildings subjected to earthquake loading.

[1] Department of Civil Engineering and Architecture, University of Pavia, Via Ferrata 3, 27100 Pavia, Italy
[2] Modelling and Structural Analysis Konsulting (MOSAYK), Piazza Castello 19, 27100 Pavia, Italy
[3] European Centre for Training and Research in Earthquake Engineering (EUCENTRE), Via Ferrata 1, Pavia

2. THE APPLIED ELEMENT METHOD (AEM) AND THE MODELLING OF MASONRY STRUCTURES

Due to space constraints, a literature review of available discrete element methods, and of how the AEM compares and differs from them, could not be included here, but may nonetheless be found in Malomo (2018) and Malomo et al. (2018).

2.1. Formulation Overview

According to the Applied Element Method (AEM) procedure a given structure is modelled through discretisation in a virtual assembly of small rigid units, carrying only mass and damping of the system, connected by springs (see Figure 1, below).

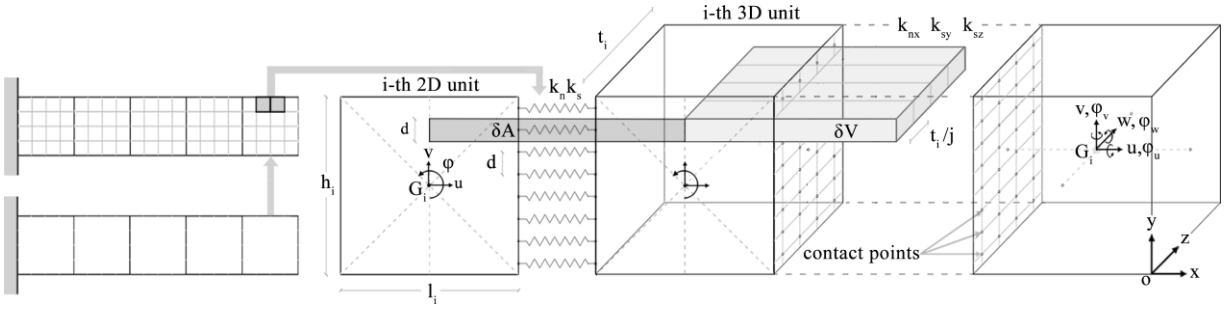

Figure 1. AEM: multi-scale discretisation of plane element and domain influence of a set of springs in 3-D space

The *i*-th plane unit is represented by a control point G_i, located in its geometrical centroid, and by a set of contact points that are uniformly distributed along the element edges. Two adjacent units are assumed to be connected at contact points by a pair of normal and shear springs (implemented with linear or nonlinear constitutive laws). Given that each group of springs completely describes stresses and deformations of a certain area δA, the behaviour of the whole assembly is deformable.

Each unit is characterised by three degrees of freedom (u,v,φ), representing its rigid body motion. Naturally, the total amount of degrees of freedom of a given model is $3n$, where n represents the number of units considered. Each normal, k_n, and shear, k_s, spring stiffness is quantified respectively using Equation (1), which involve geometrical parameters, such as the length l_i and the thickness t_i, modelling values such as the distance d between two consequent springs, and the elastic material properties E (Young's modulus) and G (shear modulus).

$$k_n = \left(\frac{E\ d\ t_i}{l_i}\right), \quad k_s = \left(\frac{G\ d\ t_i}{l_i}\right) \tag{1}$$

2.2. Formulation for masonry structures

Within the framework of AEM modelling of URM structures, an arbitrary masonry segment is composed of brick elements connected to each other by equivalent springs, in which the mechanical properties of brick-mortar interfaces (see Figure 2) are lumped (i.e. no additional DOFs are assigned to mortar layers). A given brick can be modelled as a rigid block or as an assembly of units; if it is desired to model potential splitting or crushing of bricks, then the latter need necessarily to be discretised).

From a computational viewpoint, two different stiffness matrices are needed here: for the brick elements assembly, since the springs connect elements of identical material, $[K_{bg}]$ is composed of the brick stiffnesses k_{nb} and k_{sb} only (Equation 2), whereas for the interfaces, $[K_{ig}]$ is made up inferring the equivalent stiffnesses k_{ni} and k_{si} (which, as indicated in Figure 2 and Equation 3 are obtained assuming the brick and mortar springs arranged in series at an arbitrary contact point).

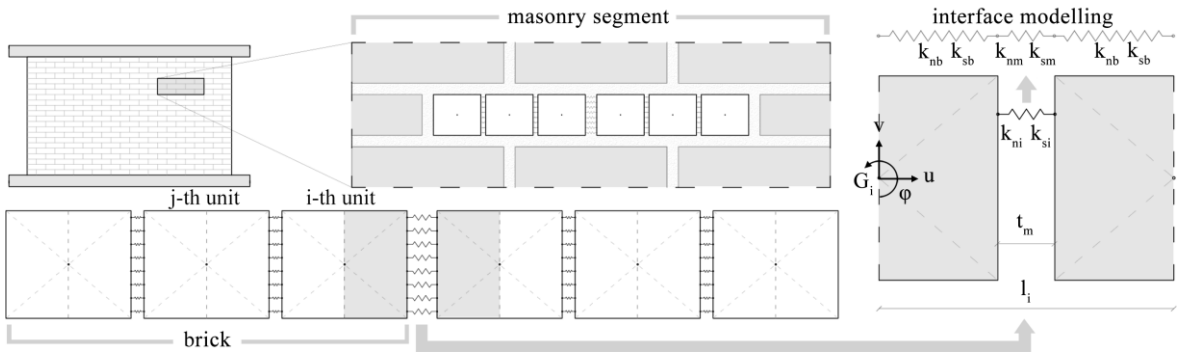

Figure 2. AEM: discretisation of a masonry segment

$$k_{nb} = \left(\frac{E\ d\ t_j}{l_j}\right), \quad k_{sb} = \left(\frac{G\ d\ t_j}{l_j}\right) \tag{2}$$

$$\frac{1}{k_{ni}} = \left(\frac{l_i - t_m}{E_b\ d\ t_i} + \frac{t_m}{E_m\ d\ t_i}\right), \quad \frac{1}{k_{si}} = \left(\frac{l_i - t_m}{G_b\ d\ t_i} + \frac{t_m}{G_m\ d\ t_i}\right) \tag{3}$$

The above parameters, representing the brick-mortar interaction, take into account both the brick and the mortar elastic properties. Naturally, in a post-cracked response stage, the elastic parameters implemented are modified according to the material constitutive laws. The AEM employs these criteria changing the stiffness values at each loading step, taking into account the damage evolution; when a given amount of springs has failed and their stiffness is set to zero, contact between units is lost.

2.3. Employed software tool

The Extreme Loading for Structures (ELS) is a commercial structural analysis software tool developed by ASI (2017) and was employed to carry out the nonlinear dynamic analyses described in this paper.

3. MODELLING SHAKE-TABLE TESTING OF THREE FULL-SCALE URM BUILDINGS

3.1. Two-storey URM terraced house (EUC-BUILD1)

This specimen was built and tested on the shake-table of Eucentre (Pavia, Italy), and consisted of a full-scale two-storey building (Figure 3) with a timber roof and RC slabs, 5.82 m long, 5.46 m wide and 7.76 m tall, for a total mass of 56.4 t. The walls, supported by a steel-concrete composite foundation, consisted of two unreinforced masonry leaves; an air gap of 80 mm was left between them, as usually seen in common practice, whilst steel ties with a diameter of 3.1 mm and a length of 200 mm were inserted in the mortar layers during construction, ensuring the connection between the two masonry leaves. The two gables in the transverse façades (East and West) supported a 43° pitched timber roof.

The inner loadbearing leaf was made of calcium silicate (CS) bricks whereas the external leaf was a clay brick (CL) veneer without any loadbearing function. The inner CS masonry was continuous along the entire perimeter of the house, while the outer clay brick leaf was not present in the South façade. It is noteworthy that the slab was not directly supported by the CS longitudinal walls; the gap between the slab and the inner CS longitudinal walls was filled with mortar after the removal of the temporary supports and the attainment of the slab's deflection resulting in almost no vertical load being transmitted to the longitudinal walls under static conditions. Further information on this specimen, including construction details and material properties can be found in Graziotti et al. (2015, 2017).

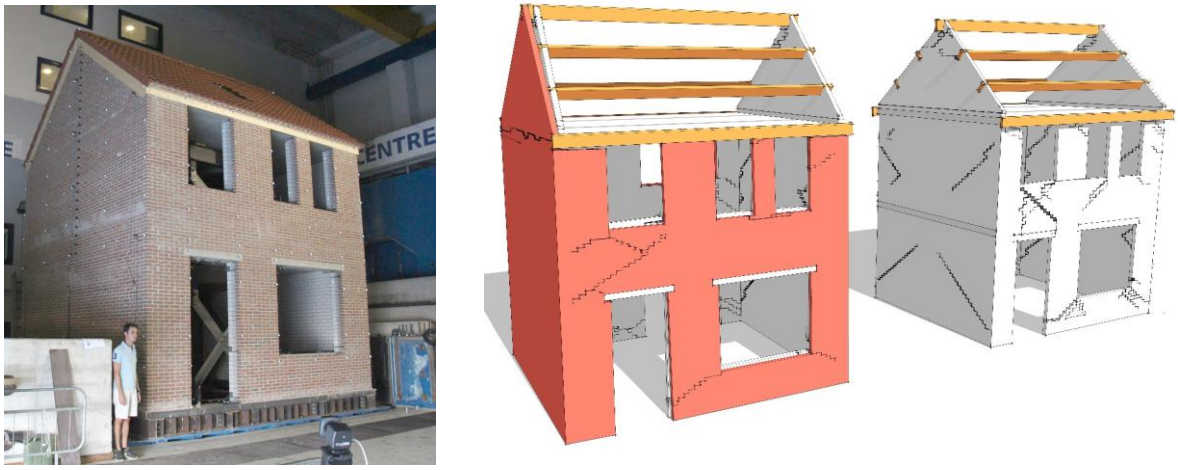

Figure 3. EUC-BUILD1: shake-table test specimen and corresponding damage pattern at end of testing on both outer-leaf clay walls and inner-leaf calcium-silicate walls (Graziotti et al. 2015, 2017)

The specimen was subjected to incremental dynamic testing, i.e. a series of shake-table runs under input motions of increasing intensity up to near-collapse of the structure. Two different ground motions, herein named EQ1 and EQ2, were employed in these tests (again, refer to Graziotti et al. 2015, 2017 for further details), with the building sustaining shaking of peak ground acceleration (PGA) of 0.14g (EQ1@150%) with no visible damage, and reaching instead a near-collapse state under the EQ2@200 test run, exhibiting the damage pattern shown in Figure 3.

Table 1 summarises the most relevant modelling assumptions made when developing EUC-BUILD1's AEM numerical model. Particularly noteworthy is perhaps the issue of the connections between wall elements; three different geometries for such connections were studied, with a 45° wall-to-wall interface joint (see Figure 4c) being found to be that leading to best results. Interested readers are referred to the report by Mosayk (2017b) for further details on this and all other modelling issues, including the calibration of constitutive relationship employed to model ties, nails and anchors.

Table 1. EUC-BUILD1: main modelling assumptions

Structural component/detail	Corresponding modelling assumption
Masonry discretisation	Rigid units and dimensionless mortar layers assembly
Boundary conditions	Structure connected through a mortar interface to a fixed slab
Roof diaphragm	Nailed connection between planks and beams modelled as equivalent spring interfaces characterised by an elastic-perfectly-plastic behaviour
Wall ties	Elastic-perfectly-plastic link elements
First floor slab-front/back inner leaves connection	Mortar interface
Second floor slab-front/back inner leaves connection	Weak mortar interface (since the gap between the slab and the wall was filled after the temporary supports removal, i.e. after RC slab deflection)
Timber beam-front/back outer leaves connection	Weak mortar interface (since the gap between the slab and the wall was filled after the temporary supports removal, i.e. after RC slab deflection)
First and second floor slab and end/party walls connection	Mortar interface
Connection between roof girders and end/party walls	Mortar interface plus elastic-perfectly plastic L-steel anchors
Wall-to-wall connection	45° connections between adjacent walls (Figure 4c)

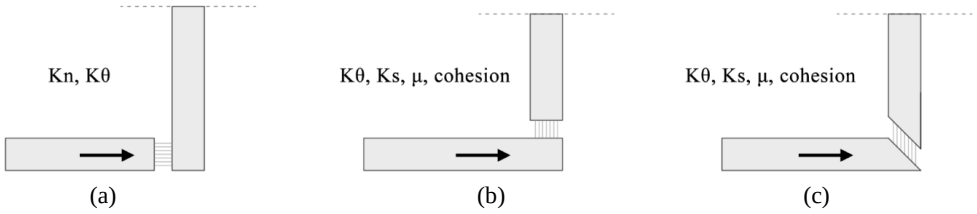

Figure 4 AEM: different types of wall-to-wall connections that may be adopted

In Figure 5(a), the maximum horizontal drifts at the attic floor level recorded for each test run are plotted against the latter PGA values, and compared with their corresponding numerical counterparts. In Figure 5(b), on the other hand, the experimental and numerical base shear vs. attic displacement hysteretic curves are compared. Finally, in Figure 6, the numerical deformed shape at instant of peak response displacement is shown.

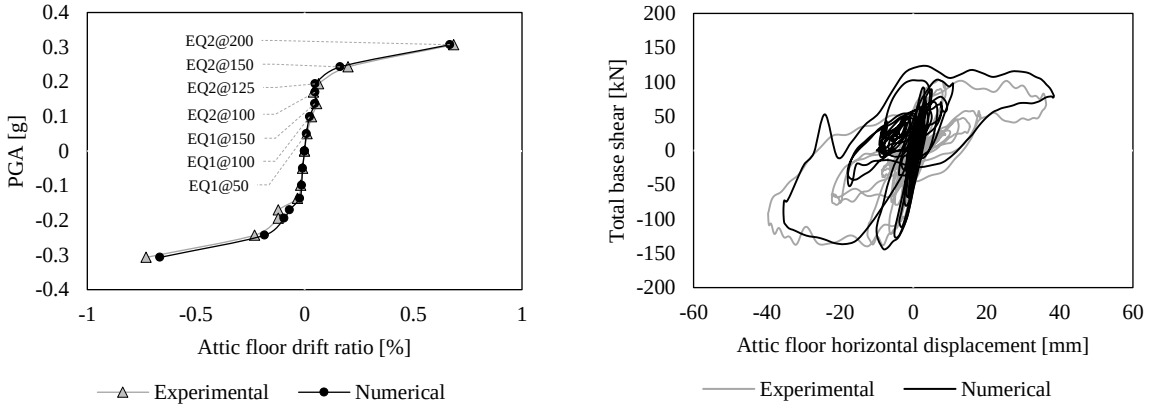

Figure 5. EUC-BUILD1: (a) PGA-Drift envelope of incremental dynamic tests/analyses, (b) experimental vs. numerical hysteretic plots (grey is experimental and black is numerical)

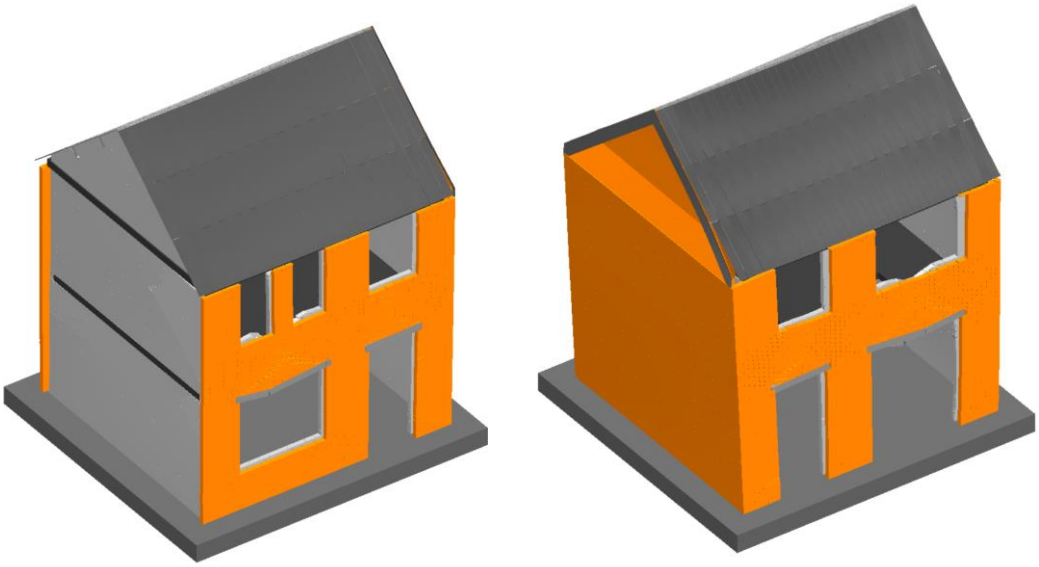

Figure 6. EUC-BUILD1: deformed shape of AEM model at instant of peak deformation (magnified x5)

3.2. One-storey URM terraced house (LNEC-BUILD1)

This specimen, built and tested on the shake-table of LNEC (Lisbon, Portugal), is a full-scale one-storey building with a timber roof and RC slab, corresponding to the second floor and roof of the EUC-BUILD1

(considered in Section 3.1 above); it was thus 5.82 m long, 5.46 m wide and 4.93 m tall, for a total mass of 31 t. The seismic input introduced at the base of LNEC-BUILD1 specimen corresponded to the floor accelerations that had been recorded during the EUC-BUILD1 test, with the exception of the final test run, which corresponded to levels of acceleration that had not been reached during such first experiment, and which led to the collapse of the structure (Figure 7). Further details on the specimen and its response can be found in Tomassetti et al. (2017).

Figure 7. LNEC-BUILD1: damaged specimen at end of testing (Tomassetti et al., 2017)

Table 2 summarises the most relevant modelling assumptions made when developing LNEC-BUILD1's AEM numerical model. It is also noted that, as in the case of EUC-BUILD1, in order to decrease the computational burden, the bricks were assumed to be rigid and the number of springs was reduced, which effectively implies that mechanisms that involve the deformability of bricks, such as crushing of masonry due to the splitting of the unit, could not be taken into account (this may result in a lower prediction of energy dissipation).

Further, it is equally herein highlighted that the gravity contribution of the roof tiles was modelled through a system of lumped masses shared amongst the elements of the mesh, again with the aim at reducing the calculation steps, resulting in a potentially slightly altered acceleration demand at the roof structure. Interested readers are referred to the report by Mosayk (2017c) for further details on the development of the model.

Table 2. LNEC-BUILD1: main modelling assumptions

Structural component/detail	**Corresponding modelling assumption**
Masonry discretisation	Rigid units and dimensionless mortar layers assembly
Boundary condition	Structure connected through a mortar interfaces to a fixed slab
Roof diaphragm	Nailed connection between planks and beams modelled as equivalent spring interfaces characterised by an elastic-perfectly-plastic behaviour
Wall ties	Elastic-perfectly-plastic beam elements
Attic floor slab and front/back inner leaves connection	Mortar interface (active after the static/gravity loading stage)
Timber beam and front/back outer leaves connection	Mortar interface (active after the static/gravity loading stage)
Attic floor slab and end/party walls connection	Mortar interface
Connection between roof girders and end/party walls	Mortar interface plus elastic-perfectly plastic L-steel anchors

In Figure 8(a), the maximum horizontal drifts at the attic floor level recorded for each test run are plotted against the latter PGA values, and compared with their corresponding numerical counterparts. In Figure 8(b), on the other hand, the experimental and numerical base shear vs. attic displacement hysteretic curves are compared. Whilst it can be seen from the latter plot that the AEM model was not able to adequately reproduce the final wider cycles of vibration (it is worth noting that the in-plane energy dissipation of the last cycle of both CS and CL longitudinal walls has been underestimated by the model), Figure 9 shows that nonetheless the collapse mode of the specimen (shown in Figure 7 above) was fully captured by the model (at the very same base level intensity as during the test).

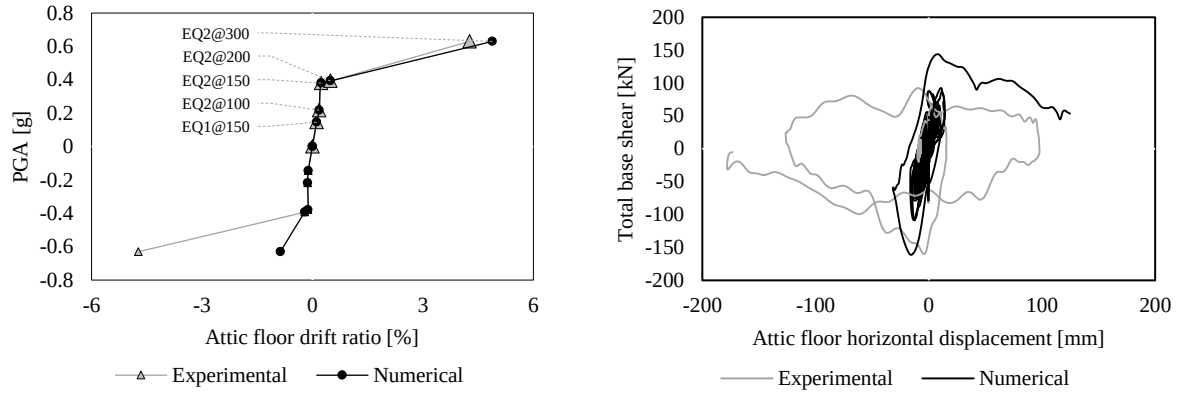

(a) (b)

Figure 8. LNEC-BUILD1: (a) PGA-Drift envelope of incremental dynamic tests/analyses, (b) experimental vs. numerical hysteretic plots (grey is experimental and black is numerical)

Figure 9. LNEC-BUILD1: specimen collapse mode as reproduced by AEM model

3.3. URM detached house (EUC-BUILD2)

This specimen was built and tested on the shake-table of Eucentre (Pavia, Italy), and consisted of a full scale building featuring construction details typical of Dutch terraced houses built before the 1940s, including the so-called Dutch cross brickwork bond. It is therefore a two-storey double-wythe clay masonry building with timber floor diaphragm and timber roof. The roof is comprised of roof trusses that span perpendicular to the direction of motion. The timber roof boards support ceramic tiling. Dimensions of the structure are 5.8 m in the North-South direction (i.e., shaking direction) and 5.3 m in the east-west direction, while the building height is 6.2 m. Further, the specimen was designed to include large asymmetrical openings on all sides and a re-entrant corner (see Figure 10), causing a discontinuity in one of the perimeter walls with the intention to magnify torsional effects under uniaxial seismic excitation. Further details can be found in Graziotti et al. (2016).

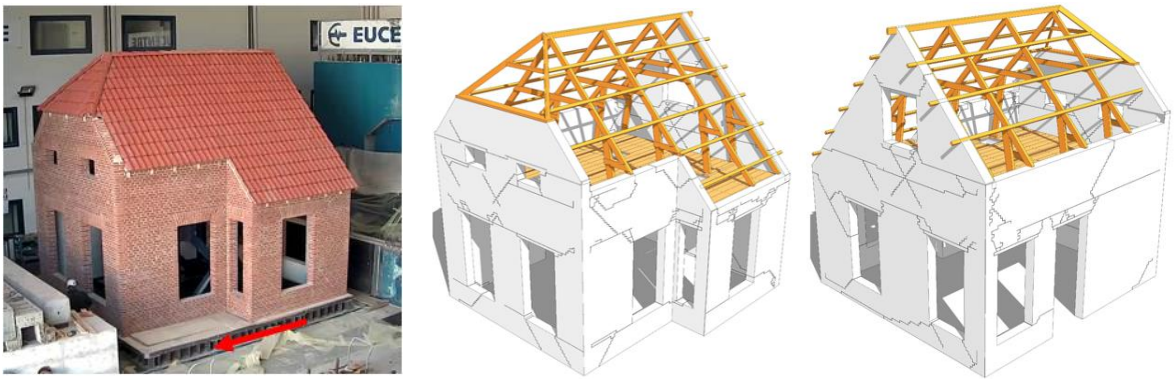

Figure 10. EUC-BUILD2: shake-table test specimen and corresponding damage pattern at end of testing (Graziotti et al., 2016)

Similarly to the previous two tests, the specimen was subjected to incremental dynamic testing with input motions representative of induced seismicity scenarios for the Groningen region (see Graziotti et al. 2016). The building suffered only minor damage under the input motion with PGA of 0.23 g and reached its near-collapse state for a PGA value of 0.68 g (with the damage pattern shown in Figure 10).

Table 3 summarises the most relevant modelling assumptions made when developing EUC-BUILD2's AEM numerical model, from where it can be gathered that a roof modelling strategy different from that employed in the previous models was herein adopted; rather that modelling each plank separately, accounting both for nails slip, rigid rotation, flexural and shear deformation of the plank elements, the roof of EUC-BUILD2 was instead modelled by means of an equivalent membrane element (Brignola et al., 2008) that intrinsically attempts to account for the abovementioned roof response components.

It is also noted that, for modelling simplicity, and given that it appeared to have negligible influence on the analyses' results, the Dutch cross brickwork modelled was not explicitly modelled. Finally, interested readers are referred to the report by Mosayk (2017b) for further details.

Table 3. EUC-BUILD2: main modelling assumptions

Input	Modelling assumption
Masonry discretisation	Rigid units and dimensionless mortar layers assembly
Boundary condition	Structure connected through a mortar interfaces to a fixed slab
Roof diaphragm	Equivalent membrane elements
First-floor diaphragm/wall connection	Mortar interface
Timber beam/wall connection	Mortar interface
Connection between roof girders and wooden diaphragm	Nailed connection between membrane and beams modelled as equivalent spring interfaces characterised by an elastic-perfectly-plastic behaviour
Wall-to-wall connection	45° connections between adjacent walls (Figure 4c)
Double-leaf brickwork	The influence of cross brick arrangement was not accounted (i.e. no perpendicular bricks to the bed joints were introduced)

In Figure 11(a), the maximum horizontal drifts at the attic floor level recorded for each test run are plotted against the latter PGA values, and compared with their corresponding numerical counterparts. In Figure 11(b), on the other hand, the experimental and numerical base shear vs. attic displacement hysteretic curves are compared. In Figure 12, instead, the numerical deformed shape and damage pattern at instant of peak response displacement are shown.

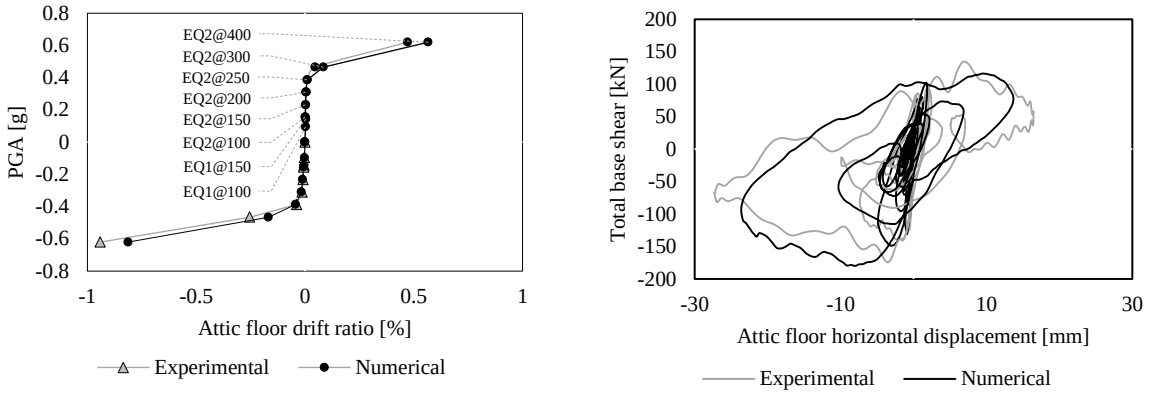

(a) (b)

Figure 11. EUC-BUILD2: (a) PGA-Drift envelope of incremental dynamic tests/analyses, (b) experimental vs. numerical hysteretic plots (grey is experimental and black is numerical)

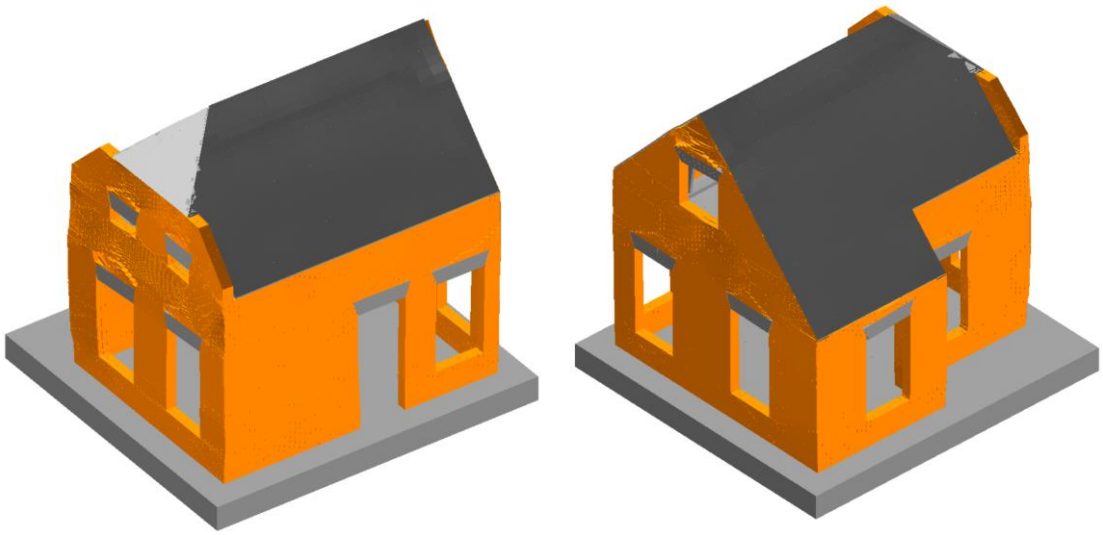

Figure 12. EUC-BUILD2: deformed shape and damage pattern of AEM model at instant of peak deformation (magnified x2)

4. CLOSING REMARKS

Three different full-scale URM house specimens subjected to earthquake loading were modelled using the Applied Element Method (AEM). This exercise confirmed the capability of the latter in analysing masonry structures under seismic excitation, independently of construction details and masonry material types.

For what concerns specimen EUC-BUILD1, the numerical results can be deemed as representative of the actual experimentally observed behaviour of the specimen. Indeed, the overall response was adequately captured, as also confirmed by comparing the numerical crack patterns of the last cycles with their experimental counterparts.

With regards to specimen LNEC-BUILD1, this endeavour also confirmed the capability of the employed modelling approach in adequately capturing the seismic response of URM buildings, given that the model did reproduce the overall structural response and the collapse of the specimen.

The numerical simulation of EUC-BUILD2 was slightly more challenging, due to the complexity of the roof structure. Indeed, the dynamic behaviour of the roof was well reproduced by the model only in the

very last stages, thus leading to a numerical response that is stiffer than the experimental one.
It is important to note that the vast majority of modelling properties adopted for the development of the post-test models coincided with their experimental counterparts, without the need for any significant adjustments to be introduced. This is further reassuring for when this modelling approach is employed in contexts where no test data is available.

Notwithstanding the above, this study also showed that further improvements are warranted, with a view to try to better capture the energy dissipation of some of the specimens, together with a better numerical reproduction of the response of the roof structures. Avenues worth exploring include:

- the possibility of adjusting, in the numerical model, the parameters that control degradation of cohesion and tensile strength (currently this is not possible, in the tool employed for these analyses);
- the feasibility of calibrating the equivalent viscous damping (currently this is not possible, in the tool employed for these analyses);
- meshing the bricks (so far modelled as rigid units), so that the energy dissipation associated to their deformation (in particular of CS bricks), cracking, splitting and crushing may be taken into account;
- better modelling the connections between wooden elements (e.g. between beam/beam and beam/plank), particularly if specific experimental data can be obtained.

5. ACKNOWLEDGMENTS

The work described in this paper was carried out within the framework of the research programme on hazard and risk of induced seismicity in the Groningen region, sponsored by the Nederlandse Aardolie Maatschappij BV (NAM). The authors also acknowledge all those at the European Centre for Training and Research in Earthquake Engineering (EUCENTRE, Pavia, Italy) and at the Portuguese Civil Engineering National Laboratory (LNEC, Lisbon, Portugal) that were involved in the testing campaign referred to in this paper, as well as the technical support staff from Applied Science International LLC (ASI), for the guidance on the use of the employed AEM software - Extreme Loading for Structures.

6. REFERENCES

Arup (2017). Typology modelling: Analysis results in support of fragility functions - 2017 batch results. Report n. 229746_031.0_REP2005. Available from http://www.nam.nl/feiten-en-cijfers/onderzoeksrapporten.html.

Arup, TU Delft, Eucentre and Arcadis, 2015. EUC-BUILD2: Modelling predictions and analysis cross validation, Report n. 229746_031.0_REP1009. Available from URL: http://www.nam.nl/feiten-en-cijfers/onderzoeksrapporten.html

Arup, TU Delft, Eucentre and Mosayk, 2017. LNEC-BUILD1: Modelling predictions and analysis cross validation, Report n. 229746_031.0_REP2004. Available from URL: http://www.nam.nl/feiten-en-cijfers/onderzoeksrapporten.html

ASI (2017). Extreme Loading for Structures v5. Applied Science International LLC, Durham (NC), USA.

Brignola A, Podestà S, Pampanin S (2008). In-plane stiffness of wooden floor, *Proceedings of the New Zealand Society for Earthquake Engineering Conference*, Wellington, New Zealand.

Crowley H, Pinho R (2017). Report on the v5 Fragility and Consequence Models for the Groningen Field. Available from http://www.nam.nl/feiten-en-cijfers/onderzoeksrapporten.html

Crowley H, Polidoro B, Pinho R, van Elk J (2017). Framework for developing fragility and consequence models for inside local personal risk. *Earthquake Spectra* 33, 1325-1345.

Graziotti F, Tomassetti U, Rossi A, Kallioras S, Mandirola M, Cenja E, Penna A, Magenes G (2015). Experimental campaign on cavity wall systems representative of the Groningen building stock. Report n. EUC318/2015U,

European Centre for Training and Research in Earthquake Engineering (Eucentre), Pavia, Italy. Available from URL: www.eucentre.it/nam-project

Graziotti F, Tomassetti U, Rossi A, Marchesi B, Kallioras S, Mandirola M, Fragomeli A, Mellia E, Peloso S, Cuppari F, Guerrini G, Penna A, Magenes G (2016). Shaking table tests on a full-scale clay-brick masonry house representative of the Groningen building stock and related characterization tests. Report n. EUC128/2016U, European Centre for Training and Research in Earthquake Engineering (Eucentre), Pavia, IT. Available from URL: www.eucentre.it/nam-project

Graziotti F, Tomassetti U, Kallioras S, Penna A, Magenes G (2017). Shaking table test on a full scale URM cavity wall building. *Bulletin of Earthquake Engineering* 15, 5329-5364.

Malomo D (2018). Scrutinising the applicability of the Applied Element Modelling in the modelling of URM structures subjected to earthquake loading. PhD Thesis, University of Pavia, Italy.

Malomo D, Pinho R, Penna A (2018). Using the Applied Element Method for modelling calcium-silicate brick masonry subjected to in-plane cyclic loading. *Earthquake Engineering and Structural Dynamics*, submitted for publication.

Meguro K, Tagel-Din H (2000). Applied Element Method for structural analysis: Theory and application for linear materials. *JSCE International Journal of Structural Engineering and Earthquake Engineering* 17, 21–35.

Meguro K, Tagel-Din H (2001). Applied Element simulation of RC Structures under cyclic loading. *ASCE Journal of Structural Engineering* 127, 1295-1305.

Meguro K, Tagel-Din H (2002). Applied Element Method used for large displacement structure analysis. *Journal of Natural Disaster Science* 24, 65-82.

Mosayk (2017a). Nonlinear dynamic analysis of index buildings for v5 fragility and consequence models. Report n. D8. Available from http://www.nam.nl/feiten-en-cijfers/onderzoeksrapporten.html

Mosayk (2017b). Using the Applied Element Method to model the shake-table testing of two full-scale URM houses. Report n. D5. Available from http://www.nam.nl/feiten-en-cijfers/onderzoeksrapporten.html

Mosayk (2017c). Using the Applied Element Method to model the collapse shake-table testing of a URM cavity wall structure. Report n. D6. Available from http://www.nam.nl/feiten-en-cijfers/onderzoeksrapporten.html

Tomasetti U, Correia AA, Graziotti F, Marques AI, Mandirola M, Candeias PX (2017). Collapse shaking table test on a URM cavity wall building representative of a Dutch terraced house. European Centre for Training and Research in Earthquake Engineering (Eucentre), Pavia, IT. Available from URL: www.eucentre.it/nam-project

van Elk J, Bourne SJ, Oates SJ, Bommer JJ, Pinho R, Crowley H (2018). A probabilistic model to evaluate options for mitigating induced seismic risk, *Earthquake Spectra*, submitted for publication.